

Received October 2, 2019, accepted October 18, 2019, date of publication November 4, 2019, date of current version November 15, 2019.

Digital Object Identifier 10.1109/ACCESS.2019.2951356

Plantar Thermogram Database for the Study of Diabetic Foot Complications

DANIEL ALEJANDRO HERNANDEZ-CONTRERAS^{ID}, HAYDE PEREGRINA-BARRETO^{ID}, JOSE DE JESUS RANGEL-MAGDALENO^{ID}, AND FRANCISCO JAVIER RENERO-CARRILLO

Instituto Nacional de Astrofísica, Óptica y Electrónica (INAOE), Puebla 72840, Mexico

Corresponding author: Hayde Peregrina-Barreto (hperegrina@inaoep.mx)

ABSTRACT The advances in infrared thermography during recent years have opened new possibilities for its use in medical diagnosis. The detection of complications related to diabetic foot is one of the many uses of this technology. This paper presents a new public plantar thermogram database composed of 334 plantar thermograms from 122 diabetic subjects and 45 non-diabetic subjects. Each thermogram includes four extra images with their respective temperature file, corresponding to the four plantar angiosomes. The database is expected to provide a valuable source to promote research about the potential of infrared thermography for the early diagnosis of diabetic foot problems. The work describes the plantar thermogram acquisition protocol, including the acquisition system and the proper preparation of the subject. It also presents a brief review of the techniques used in previous works for segmentation, registration and correction of feet posture.

INDEX TERMS Diabetes mellitus, diabetic foot, infrared thermography, thermogram database.

I. INTRODUCTION

The use of infrared thermography (IRT) in medical imaging diagnosis has increased in recent years as a result of technological advances in infrared cameras to improve the speed of response and resolution [1]. IRT is a non-contact, non-intrusive and non-invasive technique that allows real time surface temperature to be displayed. In contrast with other imaging techniques used in medicine, IRT does not use any harmful radiation since it only detects the radiation emitted by the object [2]. In the case of diabetes, IRT has been successfully used, especially to detect complications related to diabetic foot [3]–[8].

Diabetic foot is one of the major complications experienced by diabetic patients, and it can be defined as the group of syndromes in which the existence of neuropathy, ischemia and infection cause tissue damage or secondary ulcers to micro-traumatisms, causing an important morbidity that can result in amputations [9]. Diabetic patients have around 12–25% lifetime risk of developing a foot ulcer [10], which is mainly related to peripheral neuropathy, and often with peripheral arterial disease [11]. As the skin can be considered an interface between the body and the environment, it can be influenced by several external and internal factors [12].

The associate editor coordinating the review of this manuscript and approving it for publication was György Eigner^{ID}.

Peripheral vascular disease (PWD) is a significant complication of diabetes and can produce changes in blood flow that will induce a change in skin temperature. An increase in skin temperature can also indicate tissue damage or inflammation associated with some type of trauma or excessive pressure. These traumas are often related to moderate repetitive stress that goes unnoticed due to sensory damage (diabetic neuropathy). Shoe-related trauma, high plantar pressures caused by foot deformities, and repetitive stress associated with walking or daily activities have been identified as the most frequent precursors of ulceration [13]. The application of thermal imaging for the detection of diabetic foot complications is based on the assumption that a variation in the plantar temperature is associated with these types of complications.

Currently, there is wide research concerning the automatic identification of diabetic foot problems using IRT. Asymmetric temperature analysis is the most common approach due to its simplicity and its consists in comparing the temperature of one foot with its contralateral. Due to the different foot shapes among subjects and the different temperatures present in diabetic patients, thermogram processing, including the segmentation process, is an important step since the accuracy of the subsequent analysis depends directly on it. Different techniques have been presented for the processing of plantar thermograms, including segmentation techniques, such as

thresholding, active contour models, edge detection, diffuse clustering, among others.

The main purpose of this paper is to present a new plantar thermogram database created during our research. To our knowledge, there is no freely available public database of plantar thermograms. The database contains 334 individual foot thermograms from 122 diabetic subjects and 45 non-diabetic subjects. The foot is isolated from the rest of the thermogram background and manually corrected to work directly with it. This public database aims to increase research about the potential of IRT for the early diagnosis of diabetic foot problems, allowing the development of more powerful techniques to detect these problems. Each thermogram includes four extra images with their respective temperature file, corresponding to the four plantar angiosomes. An angiosome is a unit composed of tissues supplied by a single artery [5], and therefore, provides valuable information that relates temperature to arterial damage. With the angiosome extraction, it may be possible to identify if the blood supply of a particular angiosome is compromised, and if it is detected, the patient can pay more attention to prevent the formation of diabetic foot ulcers [5]. Also, for each sample, the foot temperature and the temperature of each angiosome are included, as well as the thermal change index (TCI). This will allow researchers to work directly with this data, if necessary.

The remainder of the paper is organized as follows. Section II presents a brief description of the different methods proposed for the segmentation and registration of the plantar thermograms. In Section III, the plantar thermogram acquisition protocol, including the acquisition system, subject preparation, subjects information, thermogram processing and angiosome extraction, is presented. Section IV presents a description of the database, and finally, in Section V the conclusion of this paper is presented.

II. RELATED WORK

IRT is a widely used technique in several medical applications, including in the detection of diabetic foot problems. The thermal analysis presented until now can be classified into four categories: independent limb temperature analysis, asymmetric analysis, temperature distribution analysis and external stress analysis [14]. Independent limb temperature analysis is a simple analysis that allows obtaining representative temperature ranges among different study groups. External stress analysis consists in applying an external stimulus to the patient and analyzing the behavior of the plantar temperature to this stimulus. The main purpose of the temperature distribution analysis is to evaluate mainly the way in which the temperature is distributed and not its magnitude. Asymmetric analysis is the most common analysis; it compares the plantar temperature of one foot with respect to the contralateral foot temperature.

Several of these analyses include automatic processes of segmentation, registration and correction of feet posture, especially asymmetric analysis. Image segmentation is the process of partitioning a digital image into a set

of non-overlapping regions, whose union is the entire image [15], whereas image registration is the process of overlaying two or more images of the same scene taken at different times, from different viewpoints, and/or by different sensors [16]. Both processes require an effective performance since the accuracy of subsequent analyses depends directly on both. In this section, a brief description of the different techniques proposed for the segmentation, registration and feet posture correction of plantar thermograms is presented.

In [17]–[22], examples of a histogram-shape based thresholding method to extract the plantar region directly from the thermogram are presented. For subsequent analysis in [18], [19], [21], [22], the feet posture was corrected by two reference points: one at the tip of the first toe and the other one at the center of the calcaneal base. After several tests, they concluded that an angle $\approx 85^\circ$ on the inside of the foot, between both points, indicated a vertical feet position. Kaabouch *et al.* [23]–[27] tested different methods for extracting the feet from the background, such as methods based on histogram shape, clustering, entropy, object attribute, as well as genetic algorithms; it was concluded that the genetic algorithm-based thresholding technique has the best results. To adjust the left and right feet at the same position for an asymmetric analysis, [24]–[27], a geometric transformation was needed. Based on two feature points, the centroid and the furthest point from the centroid to the heel, the angle was calculated with the line between the two points and the vertical direction. Then, a translation to put the feet in the middle of the image and a rotation to the vertical position of the characteristic line were preformed. In [23], the same author presented an alternative technique based on scalable scanning. The proposed technique allows a more reliable comparison, even if the shapes and sizes of the two foot projections are different.

Thresholding methods achieve good results when the contrast between the plantar region and background is high. This produces a bimodal image histogram where two data peaks can be observed, one representing the plantar region and the other representing the background. In 2013, Liu *et al.* [28] implemented the methods described in [23]–[27], but the results obtained were not satisfactory in image, where there is no clear intensity difference between the foot and the background. They implemented the Active Contours Without Edges (ACWE) method; however, the images without high contrast and visible parts of the ankles and legs still needed manual adjustment. In [34], they developed a computer-aided diagnostic system for diabetic peripheral neuropathy, where the segmentation process was based on techniques, such as continuous max-flow, model based segmentation, shape preservation, convex hull, and temperature normalization. First, they applied the continuous max-flow method to segment the foot in the first frame of the thermal video. With the segmentation of the first frame, they applied a shape extraction to create a geometric foot model. Then, for the successive frames, a numerical optimization was used to search for the best fit of the foot model based on mutual information. Only rotation and translation were needed because

the authors mentioned that there was a minimum deformation of the foot, and the foot did not warm up uniformly. After this process, they extracted the temperature change for each point on plantar temperature to analyze it with their thermal model and obtained a thermoregulation map at each point of the feet.

In [30], a comparison between two image segmentation techniques for plantar thermograms is presented. The edge detection and watershed method were used to segment ten thermograms of healthy feet and ten of diabetic feet. The comparison shows that the edge detection technique was more reliable than the watershed method. More recently, Sudha *et al.* [43] presented a semi-automatic segmentation algorithm based on Otsu thresholding, followed by morphological operations. They tested this methodology under three different image acquisition setups. They showed that morphological operations combined with the Otsu thresholding performed good results in each of the image conditions, mainly in the ankle area. In a subsequent work [44], they used the same segmentation method presented in [43] for healthy foot thermograms, but they used an ACWE method for diabetic foot thermograms. In [46], a method based on a modified active contour that included prior shape information, namely an atlas of the plantar foot contour, is presented. The proposed method overcomes the classical Snake method, as well as other segmentation methods, such as region growing, active contour approaches, methods based on level sets [48]–[50] and the graph cut approach [51]. However, as in other works, the problem also occurs when the toes are cold or at the same temperature as the background.

Despite the different methods presented to isolate the plantar region directly from the thermogram, the main problem occurs when the temperature of a part of the foot is similar to the background, so the contrast between both regions is low. To avoid this problem, Liu *et al.* [40] presented a more precise foot segmentation when there is no clear thermal contrast between the foot and the background. This was done by using the color image to guide the thermogram segmentation. They used three different unsupervised learning algorithms to extract the feet of the color images: the K-means algorithm, the expectation-maximization linear discriminant classifier (EM-LDC) and the expectation-maximization linear quadratic classifier (EM-QDC). The algorithms were applied in six different color planes (RGB, normalized RGB, RGB-ratio, HSV, CIE L*a*b*, and YCbCr) and with different values of k ($k = 1, 2, 3$). Of the 72 possible combinations, only nine satisfied their performance requirements, from which they chose segmentation in the CIE Lab plane, using the EM-LDC algorithm with $k = 3$ with a sensitivity and specificity of 97.9 ± 0.7 and 98.9 ± 0.7 , respectively. The next step is the alignment of the RGB and thermal image. To do this, they selected a quantitative criterion based on the observation that statistics of the temperatures in a region inside the foot differ when compared with a region outside of the foot. Finally, to perform the asymmetric analysis, a landmark-based deformation model with B-splines was implemented. In [41], it is mentioned that segmenting the feet directly

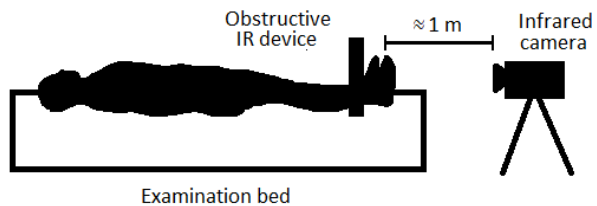


FIGURE 1. Components of the acquisition system: an examination bed, an obstructive IR device and the infrared camera.

from the thermogram is more complex than hands and shins because the feet are typically colder, and the temperature difference between the feet and the background can be very small, making several segmentation processes ineffective. For this reason, they also used the RGB image to segment the feet by a thresholding method. The registration process was performed using the inbuilt MATLAB function `imregister()` with a maximum number of iteration of 300. This function performed an intensity-based image registration. Recently, in 2019, Verma *et al.* [47] carried out a comparison between different segmentation techniques, presenting the advantages and disadvantages of each of these methods: thresholding methods (global and multiple threshold), edge based methods (Sobel, Canny and Roberts operators), region based methods (region growing and region splitting and merging), watershed, and clustering based methods (hard and soft clustering). Table 1 summarizes the different methods proposed for segmentation and registration of plantar thermograms.

III. PLANTAR THERMOGRAM ACQUISITION PROTOCOL

Currently, the database is composed of 167 plantar thermograms, which were obtained from 122 diabetic subjects and 45 non-diabetic subjects. The subjects were recruited from the General Hospital of the North, the General Hospital of the South, the BIOCARE clinic and the National Institute of Astrophysics, Optics and Electronics (INAOE) over a period of 3 years (from 2012 to 2014). All of these places are located in the city of Puebla, Mexico. The participants were informed about the tests and voluntarily agreed to participate in the study. In order to obtain accurate and useful thermograms for clinical practice, the recommendations of the International Academy of Clinical Thermology were followed [54].

A. ACQUISITION SYSTEM

The system consists of three main components: an examination bed, an obstructive IR device and the infrared camera (Fig. 1). The first component is an examination bed used to keep the subject in supine position during the acclimatization period (see Section III-B). The second component is an obstructive IR device to isolate the plantar temperature. The device was placed in the malleolus area to avoid the radiation emitted from the rest of the body. Several modifications were made to the obstructive IR device to get a better contrast between the plantar region and the background. The final device is a metal plate with two holes to place the feet. A piece of black cloth is dropped on the plate to avoid any temperature

TABLE 1. Segmentation and registration methods proposed for plantar thermograms.

Author	Year	Study Group	Segmentation Methods	Image Registration
Kaabouch et al. [24]–[27]	2009–2011	Over 100 thermal images [26], [27]	Otsu method, Ridler technique [31], Kapur et al. [32], Tsai et al. [33], Genetic algorithms-based thresholding technique	Geometric Transformation: translation and rotation based on two feature points
Kaabouch et al. [23]	2012	80 images of healthy feet 60 with visible thermal abnormalities	Genetic algorithms-based thresholding technique	Scalable scanning technique
Liu et al. [28]	2013	A case study	Active contours without edges	B-spline grid, non-rigid point-based registration (Klein et. al [53])
Chekha et al. [29], [34]	2013–2014	40 subjects	Continuous max-flow method [34]	Semi-automatic approach based on cross-correlation [29] Model based on mutual information [34]
van Netten et al. [35]	2014	54 diabetic patients	Active contours without edges [36]	
Vilcahuaman et al. [37], [38]	2014–2015	85 diabetic subjects [38] 82 diabetic subjects [37]	Chan and Vese active contour algorithm	Iterative closest point method
Vilcahuaman et al. [39]	2015	2 subjects	Fuzzy clustering and growing seeds	Iterative closest point method
Liu et al. [40]	2015	37 diabetic subjects	K-means clustering and expectation-maximization (EM) clustering on six color representations: RGB, normalized RGB (rgb), RGB-ratio, HSV, CIE L*a*b*, and YCbCr	Landmark based deformation model with B-splines
Hernandez et al. [17]–[22]	2015–2019	24 non-diabetic and 20 DM subjects [20] 30 non-diabetic and 30 DM subjects [17] 40 non-diabetic and 100 DM subjects [19]. 35 non-diabetic and 100 DM subjects [18] 35 non-diabetic and 111 DM subjects [22]	Histogram shape-based thresholding method	
Nandagopan et al. [30]	2016	10 normal foot thermal images 10 diabetic foot thermal images	Edge Detection and watershed technique	Landmark based deformation model with B-splines
Gaucci et al. [41]	2016	11 test images	Thresholding method in RGB image	Intensity-based image registration
Fraiwan et al. [42]	2017		Otsu method	Intensity-based registration
Sudha et al. [43]	2017	36 thermal images	Otsu thresholding followed by morphological operations	Intensity-based registration
Etehad tavakol et al. [45]	2017	59 thermographic images	Snake algorithm [52]	
Bougrine et al. [46]	2017	50 plantar foot thermal images	Snake Atlas-based method	
Sudha et al. [44]	2018	62 thermal images of diabetic subjects 20 thermal images of healthy subjects	Otsu thresholding followed by morphological operations for healthy foot and ACWE method for diabetic patients	Intensity-based image registration with imregister function of MATLAB Software
Verma et al. [47]	2019	30 diabetic subjects	Thresholding (global and multiple), Edge based methods (Sobel, Canny and Roberts), region based methods (region growing and region merging and splitting), watershed, clustering (K-means)	



FIGURE 2. Final obstructive IR device.

TABLE 2. Demographic Information of both groups.

	Control Group	DM Group
Volunteers	45	122
Female	16	89
Male	29	33
Age(years)	27.76 ± 8.09	55.98 ± 10.57

outside the plantar region. Thus, a uniform background is obtained in the color image for a better segmentation (Fig. 2).

Finally, the third component is the infrared camera. Two different infrared cameras were used for thermogram acquisition (FLIR E60 and FLIR E6). During the thermogram acquisition, the position of the camera is fixed by an adjustable vertical tripod to avoid any undesirable movement. The tripod is placed one meter away from the feet.

B. SUBJECT PREPARATION

Before the acquisition process, all patients were informed of the study to obtain their verbal consent to participate. Also, all patients were asked if they had prolonged sun exposure or if they perform any intense physical activity. If any of these answers were affirmative, they were re-scheduled for another day to conduct the study.

The preparation of the subjects was done in a room with a temperature of 20 ± 1 °C. The participants were asked to remove their shoes and socks and clean their feet with a damp towel. After that, the subjects were invited to maintain a supine position for 15 minutes in order to reach a state of thermodynamic equilibrium and to improve the accuracy of temperature variation detection [55]. During resting time, the feet remained uncovered and the patients had to avoid any type of effort that could affect blood pressure, and as a result, affect the plantar temperature. This is the reason why no type of device was used to maintain the correct position of the feet.

C. SUBJECT INFORMATION

During the acclimatization period, personal information about the patient was taken, such as name, age, gender, height and weight. Table 2 summarizes the data collected.

D. THERMOGRAM PROCESSING

For each plantar thermogram, the left and right foot were extracted, and each was taken as a separate thermogram,

obtaining a database of 334 individual thermograms. As mentioned previously, if any device is placed to maintain the feet in vertical position, the blood pressure can be affected, and therefore, the temperature will also be affected. for this reason, after segmenting the feet, the posture was digitally corrected.

Figure 3 shows some examples of the segmentation performed in plantar thermograms with different methods: Otsu thresholding, Chan and Vese method and canny detector. As mentioned in Section II, if there is a significant difference between the temperature of the plantar region and the background, most of the segmentation techniques present an effective performance (Figs. 3a-d). However, there may be cases in which the plantar temperature is almost the same as the background temperature (Figs. 3e and i), which is why the segmentation techniques are ineffective (Fig. 3f-i). This is the reason why the segmentation directly on the thermogram has been a problem addressed in different works. Figure 4 shows the segmentation performed on the RGB image under different segmentation techniques: expectation-maximization algorithm, k-means and canny detector. Using the device mentioned in Section III-A, the piece of black cloth over the device allows us not only to create a contrast between the plantar region and the background, but also to cover the ankle and part of the foot without creating unnecessary pressure. It can be seen that the best results are obtained by the canny edge detector.

Once the plantar region is isolated, the plantar thermograms are split into two images, one for each foot, and after that, the foot posture is corrected. Figure 5 shows the comparison between the method used in a previous work [22] (blue line) and Hotelling transform (green line). The first one is based on two reference points: the tip of the innermost toe, and the center of the calcaneal base. The angle between the line connecting the two points and a vertical line is calculated and the foot is rotated until reaching an internal angle of 85°. It can be seen that the difference between the two methods is minimal (blue and green line). The disadvantage of the first method occurs mainly when locating the two points because if there was no precise segmentation, the points could not be located properly. Several modifications of the device were made until reaching the final device, where an improvement in the segmentation of low contrast thermograms can be observed. All thermograms were checked after the automatic process of segmentation and posture correction. If the result was not satisfactory, the thermograms were manually fixed for the database.

E. ANGIOSOMES EXTRACTION

Several works have presented a thermal plantar analysis based on the measurement of specific points. If we take into account the temperature from the entire plantar region, it is possible to perform a complete analysis of its general state. However, it is important to consider a regional division of the foot since it does not have a uniform temperature [56], [57]. As reported in [5], an angiosome is a unit composed of tissues supplied

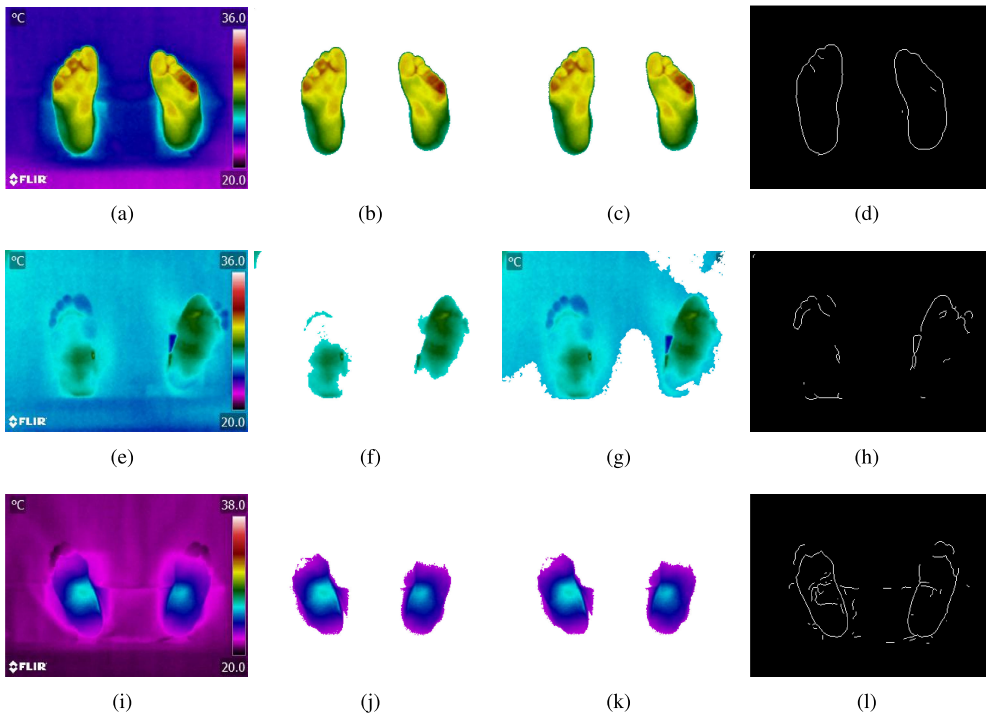


FIGURE 3. Comparison between different segmentation methods on thermogram. (a,e,i) original thermograms, (b,f,j) Otsu thresholding methods, (c,g,k) Chan and Vese method, and (d,h,l) canny detector.

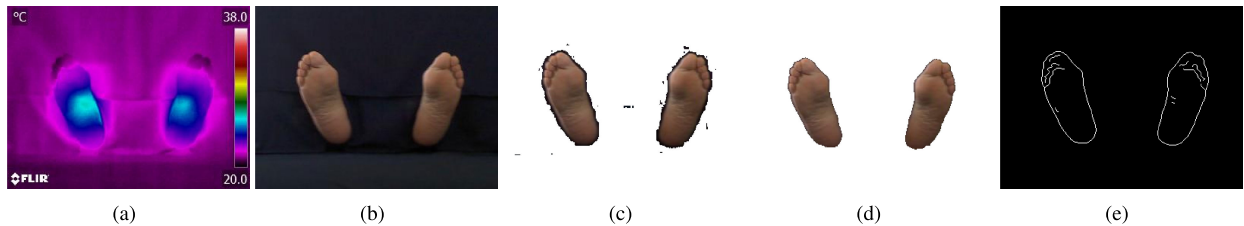


FIGURE 4. Comparison between different segmentation methods on RGB image. (a) Thermogram, (b) original RGB image, (c) expectation-maximization algorithm, (d) k-means, and (e) canny detector.

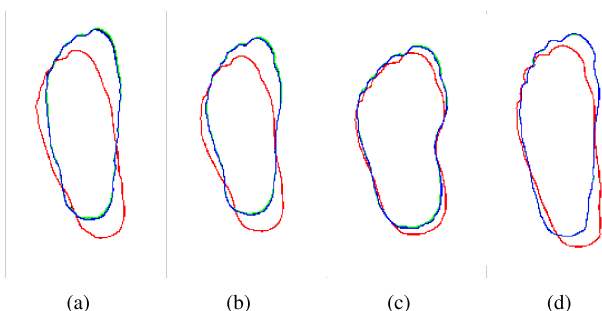


FIGURE 5. Comparison between two rotation methods. The red line is the original edge, the blue line is the rotation method proposed in [22], and the green line is the rotation by the Hotelling transform.

by a single artery, and therefore, provides valuable information that relates temperature to arterial damage. The foot is divided into four angiosomes: Medial Plantar Artery (MPA), lateral plantar artery (LPA), medial calcaneal artery (MCA) and lateral calcaneal artery (LCA) (Fig. 6). After the foot

position is corrected, angiosome division is carried out by an automatic process. To do this, a proportional segmentation was performed, as presented in a previous work [19]. Two reference points are taken to calculate the height of the foot (H): Point A is located at the tip of the innermost toe, and Point B is located at the center of the calcaneal base. The width of the foot (W) is calculated by identifying two additional points C and D, which correspond to the largest part of the foot. Once the dimensions are known, the angiosomes are extracted through a proportional division of the foot, as shown in Fig. 6. Therefore, four sub-images are created, one for each angiosome.

IV. PLANTAR THERMOGRAM DATABASE

The database contains 334 foot thermograms, each one assigned with a unique nomenclature. The first letters represent the subject group (CG: control group and DM: diabetic group) followed by three digits to number the thermograms. After that, the gender of the subject (M: male

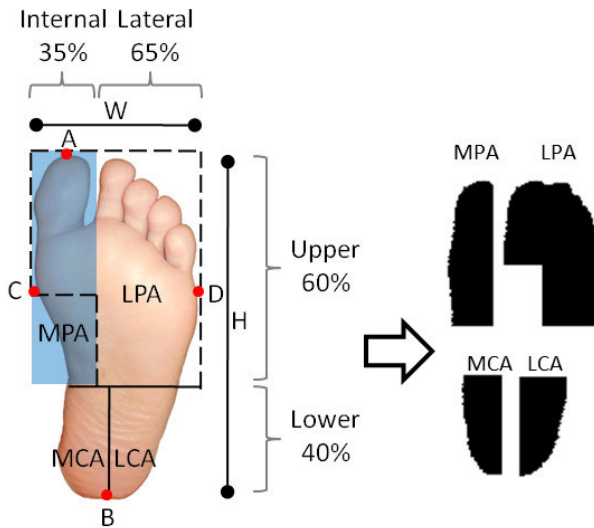


FIGURE 6. Proportional foot division into plantar angiosomes.

TABLE 3. Mean temperature values per angiosome for the control group established in [19].

Angiosome	\bar{T}	s
MPA	25.8	1.4
LPA	25.7	1.3
MCA	26.4	1.3
LCA	26.1	1.4

and F: female) is specified, and finally, the last letter indicates whether the thermogram corresponds to the left (L) or right (R) foot: *Subject Group_three digits_gender_foot*. For example, the image *DM001_F_L.png* belongs to the left foot thermogram of a woman in the diabetic group. RGB thermograms are only illustrative since these do not contain direct temperature information. That is why each thermogram includes a temperature file with a .csv extension with the same nomenclature (*DM001_F_L.csv*). In the temperature file, the plantar region is isolated as in the thermogram and contains the temperature of each pixel. For each thermogram, four images are included with the respective temperature file of each of the plantar angiosomes. The same nomenclature is used with the inclusion of three letters at the end, indicating the angiosome (*DM001_F_L_MPA.png*). The thermograms were manually corrected in case the segmentation or rotation were not adequate. In total, the database contains 1670 RGB images: 334 foot images and 1336 angiosome images (four per foot), and the same number of csv files. Figure 7 shows some examples of the plantar thermograms.

Tables 4 and 5 show the general temperature of the foot and the regional temperature divided by each angiosome of the foot. Also, the thermal change index (TCI) was calculated with the reference values established in [19] (Table 3). All values were calculated with the .csv files of the database. The TCI is based on the temperature dispersion in relation to the reference and takes into account not only the temperature difference between regions but also the temperature interval

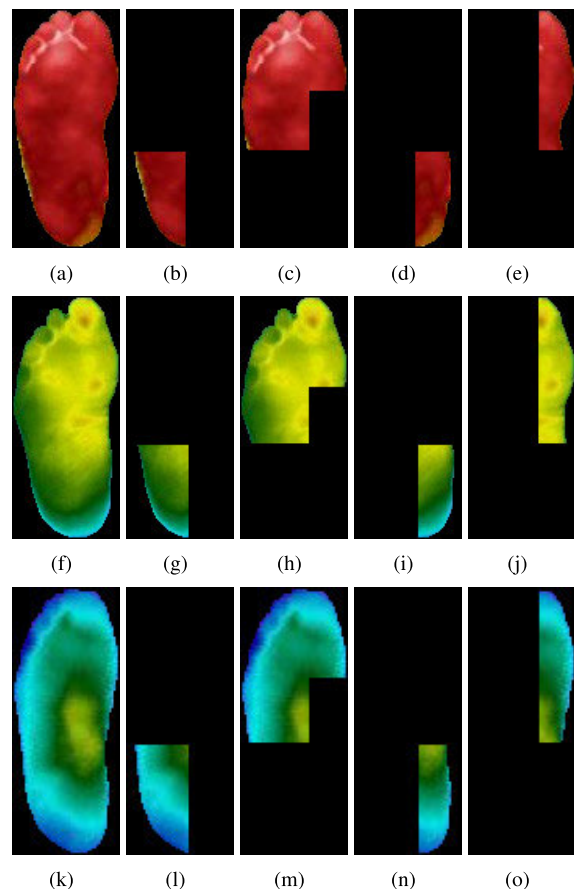


FIGURE 7. Examples of the plantar thermograms with their respective plantar angiosomes. (a,f,k) Foot, (b,g,l) MCA angiosome, (c,h,m) LPA angiosome, (d,i,n) LCA angiosome, and (e,j,o) MPA angiosome.

of the control group. The TCI value is based on the mean differences between corresponding angiosomes from a diabetic subject and the reference values from Table 3 [19]. The index is calculated by:

$$TCI = \frac{\sum |C_{ang} - DM_{ang}|}{4} \quad (1)$$

V. CONCLUSION

In this work, the design of a plantar thermogram database is presented. The database is composed of 334 individual thermograms from 122 diabetic subjects and 45 non-diabetic subjects. Each thermogram includes four extra images corresponding to the plantar angiosomes, and each image is accompanied by its temperature file. The angiosome extraction allows analyzing the temperature of these regions and can be used to identify possible changes in the angiosome blood supply that can indicate risk of ulceration. The database will allow researchers of this area to evaluate the potential contribution of the IRT for early detection of diabetic foot complications. In addition, the document presents some of the techniques of segmentation, registration and correction of feet posture presented in previous works, emphasizing the differences and problems that have not been resolved yet.

TABLE 4. Data Analysis of DM group.

Subject	Gender	Right Foot						Left Foot					
		General	LCA	LPA	MCA	MPA	TCI	General	LCA	LPA	MCA	MPA	TCI
DM001	M	32.47	32.08	32.70	32.36	32.79	6.48	32.09	31.53	32.39	31.81	32.39	6.03
DM002	M	26.99	26.54	26.95	26.84	27.38	0.93	26.33	26.39	25.93	26.75	26.45	0.38
DM003	F	28.04	28.22	27.57	29.06	27.70	2.14	27.19	26.96	26.96	27.90	27.38	1.30
DM004	M	32.32	31.67	32.54	31.86	32.61	6.17	30.71	29.78	30.96	31.04	30.72	4.62
DM005	M	24.48	24.19	24.48	24.26	24.52	1.64	25.36	24.40	25.72	24.88	25.57	0.87
DM006	F	33.04	32.54	33.42	32.36	33.22	6.88	33.61	33.38	33.82	33.43	33.66	7.57
DM007	F	29.09	28.34	29.47	28.27	29.79	2.97	27.53	27.06	27.41	27.60	27.92	1.50
DM008	M	31.60	30.21	32.37	30.65	31.62	5.21	30.07	29.22	30.54	29.32	30.56	3.91
DM009	F	29.73	29.03	30.06	29.38	29.91	3.59	30.08	29.38	30.30	30.00	30.55	4.06
DM010	M	34.70	34.16	35.01	34.32	34.78	8.57	34.31	33.76	34.58	33.82	34.55	8.18
DM011	F	31.69	31.06	32.03	31.41	31.74	5.56	31.86	31.53	32.09	31.59	32.14	5.84
DM012	F	32.08	31.38	32.48	31.52	31.90	5.82	32.81	32.63	32.85	32.92	32.30	6.68
DM013	F	28.06	28.80	27.32	29.01	27.20	2.08	27.47	27.52	26.94	27.51	28.12	1.52
DM014	F	32.39	32.31	32.38	32.42	32.78	6.47	31.70	31.06	32.02	31.14	32.17	5.60
DM015	M	33.90	33.54	34.26	33.31	33.61	7.68	33.71	33.14	33.92	33.43	34.21	7.68
DM016	F	32.78	32.51	32.93	33.00	32.39	6.71	33.05	32.98	33.15	33.27	33.10	7.12
DM017	F	31.05	29.91	31.87	29.77	32.11	4.91	30.71	28.91	31.79	29.04	31.90	4.41
DM018	M	29.70	29.44	29.77	29.37	30.41	3.75	26.77	26.86	26.58	26.73	27.63	0.95
DM019	F	31.09	30.30	31.70	29.95	31.71	4.91	31.69	31.14	32.18	30.61	32.24	5.54
DM020	F	29.89	30.17	29.54	30.40	30.04	4.04	29.95	30.19	29.78	29.68	30.13	3.95
DM021	F	31.08	30.71	31.22	30.88	30.80	4.90	29.76	29.87	29.48	29.91	29.88	3.79
DM022	F	30.72	29.13	31.67	29.04	31.09	4.23	30.70	29.67	31.21	29.80	31.14	4.46
DM023	F	29.13	26.87	30.40	27.54	30.19	2.75	30.46	28.64	31.41	29.30	31.36	4.18
DM024	M	28.72	27.55	29.41	27.86	28.99	2.45	32.43	31.10	33.20	31.38	32.81	6.12
DM025	M	32.07	30.87	32.89	30.94	32.54	5.81	32.10	30.53	32.97	31.01	33.03	5.89
DM026	M	32.35	31.85	32.62	32.13	33.00	6.40	32.34	32.54	32.29	32.52	32.22	6.39
DM027	M	32.45	31.81	32.95	31.89	32.49	6.28	31.91	31.44	32.35	31.22	32.22	5.81
DM028	M	25.26	24.76	25.19	25.11	25.71	0.81	24.19	24.15	24.05	24.14	24.43	1.81
DM029	F	27.86	27.38	27.93	27.81	28.21	1.83	29.08	28.79	28.93	29.77	29.61	3.27
DM030	F	28.42	27.74	28.62	28.03	29.53	2.48	28.25	27.87	28.20	28.42	28.78	2.32
DM031	F	30.53	30.82	30.11	31.34	29.75	4.50	31.74	30.88	32.27	31.49	31.08	5.43
DM032	M	32.31	30.01	33.87	29.82	34.14	5.96	31.13	29.46	32.15	29.33	32.51	4.86
DM033	M	25.07	25.09	24.70	24.62	25.43	1.04	23.93	23.20	23.96	23.47	25.28	2.02
DM034	F	30.85	29.42	31.42	29.98	31.50	4.58	31.42	30.21	31.85	30.68	32.11	5.21
DM035	F	28.98	28.50	29.02	29.24	29.97	3.18	30.44	29.39	31.08	29.27	31.79	4.38
DM036	M	32.37	31.10	33.03	31.69	33.31	6.28	31.83	30.49	32.75	30.33	32.59	5.54
DM037	F	24.60	24.44	24.47	24.56	24.86	1.42	24.07	24.45	23.70	24.61	24.04	1.80
DM038	F	30.04	28.79	30.75	29.04	31.01	3.90	30.33	29.04	30.96	29.35	31.09	4.11
DM039	M	31.16	30.63	31.45	30.84	31.10	5.00	30.92	30.59	31.10	30.84	30.87	4.85
DM040	F	32.53	31.78	32.85	32.25	32.87	6.44	32.18	31.94	32.24	32.21	32.25	6.16
DM041	M	31.24	30.18	31.76	30.63	31.96	5.13	31.71	30.69	32.17	31.04	32.24	5.54
DM042	F	31.15	30.84	31.21	30.89	31.50	5.11	31.09	31.15	30.91	31.15	31.39	5.15
DM043	M	29.89	29.00	30.27	28.94	30.58	3.70	31.13	29.92	31.69	30.00	32.14	4.94
DM044	F	25.95	26.39	25.63	26.51	25.51	0.19	26.57	26.19	26.59	26.34	27.32	0.64
DM045	F	30.50	30.06	30.81	30.05	30.60	4.38	30.02	29.56	30.25	29.81	30.11	3.93
DM046	M	31.89	31.05	32.36	31.32	32.38	5.78	29.75	29.65	29.64	29.87	30.19	3.84
DM047	F	33.55	33.37	33.76	33.39	33.81	7.58	32.66	32.02	32.98	32.24	33.41	6.66
DM048	F	30.71	30.51	30.55	30.83	31.40	4.82	30.84	30.18	30.94	30.64	31.33	4.77
DM049	F	28.02	27.16	28.47	27.30	28.45	1.85	27.18	26.32	27.47	27.01	27.75	1.14
DM050	F	32.17	32.21	32.10	32.35	32.44	6.27	32.09	32.33	31.83	32.51	32.40	6.27
DM051	F	28.49	28.48	28.34	28.52	29.01	2.59	29.05	28.80	29.12	28.80	29.54	3.06
DM052	F	28.64	26.97	29.44	27.53	29.54	2.37	28.56	26.77	29.38	27.47	29.52	2.29
DM053	M	27.16	27.50	26.85	27.25	26.79	1.10	25.99	25.83	25.93	26.16	25.77	0.19
DM054	F	28.84	28.35	29.22	28.17	28.92	2.66	28.85	28.25	29.23	28.45	28.92	2.71
DM055	F	31.46	31.23	31.81	30.64	32.00	5.42	31.60	31.22	31.92	30.95	31.98	5.52
DM056	F	28.71	27.70	29.17	27.78	29.66	2.58	27.40	25.70	28.16	25.87	29.07	1.66
DM057	F	27.28	27.07	27.13	27.42	27.82	1.36	32.38	32.06	32.63	32.07	32.44	6.30
DM058	F	24.03	23.97	23.91	24.20	24.03	1.97	25.86	26.64	25.35	26.82	25.34	0.44
DM059	F	32.68	32.44	32.92	32.29	32.85	6.63	32.66	31.94	32.98	32.47	32.87	6.57
DM060	F	32.12	31.95	32.16	32.40	31.80	6.08	32.00	31.15	32.57	31.23	32.23	5.79
DM061	F	26.11	26.53	25.60	26.86	25.63	0.29	25.87	26.71	25.09	27.01	25.05	0.65
DM062	M	28.29	27.56	28.55	27.93	28.56	2.15	28.24	28.54	27.80	29.31	28.10	2.44

TABLE 4. (Continued.) Data Analysis of DM group.

Subject	Gender	Right Foot					Left Foot						
		General	LCA	LPA	MCA	MPA	TCI	General	LCA	LPA	MCA	MPA	TCI
DM063	F	32.08	31.85	32.13	32.25	31.57	5.95	32.15	31.14	32.59	31.43	32.74	5.97
DM064	M	34.54	32.78	35.61	32.76	35.36	8.13	33.73	32.53	34.43	32.70	34.06	7.43
DM065	F	21.52	22.18	20.84	22.47	21.18	4.33	20.42	20.90	19.78	21.26	20.27	5.45
DM066	F	26.91	26.88	26.73	26.94	27.18	0.93	26.99	26.80	26.91	27.01	27.01	0.93
DM067	F	29.09	27.15	30.01	27.64	30.45	2.81	27.74	26.41	28.26	26.83	28.87	1.59
DM068	F	34.87	34.16	35.49	33.60	35.23	8.62	35.28	35.17	35.56	34.60	35.58	9.23
DM069	F	30.86	30.50	30.99	30.93	30.93	4.84	29.98	29.73	29.97	30.10	30.21	4.00
DM070	F	29.99	29.23	30.35	29.46	30.40	3.86	29.99	29.37	30.23	29.88	30.32	3.95
DM071	F	26.98	27.63	26.29	27.89	26.97	1.20	27.14	27.81	26.47	27.89	27.10	1.32
DM072	F	29.31	27.75	29.92	28.84	30.02	3.13	29.34	28.08	30.05	28.53	29.74	3.10
DM073	F	29.63	29.46	29.43	29.94	30.20	3.75	29.65	29.26	29.48	30.01	30.40	3.79
DM074	F	30.70	29.38	31.45	29.32	31.08	4.31	30.90	29.84	31.46	30.25	30.80	4.59
DM075	F	30.76	28.71	31.94	29.01	32.21	4.47	31.37	29.80	32.29	29.84	32.63	5.14
DM076	M	33.57	33.20	33.88	32.92	33.73	7.43	33.71	33.55	33.85	33.44	33.78	7.66
DM077	F	33.05	32.62	33.41	32.45	33.35	6.96	32.93	32.80	33.20	32.28	33.06	6.84
DM078	F	31.59	31.21	31.71	32.18	31.61	5.68	29.47	29.39	29.67	29.44	29.81	3.58
DM079	M	26.45	27.16	25.64	27.84	25.95	0.68	26.10	26.77	25.37	27.40	25.30	0.63
DM080	F	29.00	27.82	29.56	28.17	30.08	2.91	28.07	27.56	28.13	27.80	28.62	2.03
DM081	F	27.95	27.99	27.52	28.78	28.05	2.08	28.15	28.26	27.75	28.74	28.34	2.27
DM082	F	33.99	32.86	34.18	33.70	35.19	7.98	34.06	32.41	34.65	33.04	35.15	7.81
DM083	M	30.73	29.23	31.57	29.39	31.92	4.53	28.90	27.42	29.77	28.01	29.65	2.71
DM084	F	29.73	28.81	29.98	29.49	30.60	3.72	29.75	28.50	30.06	29.04	31.46	3.77
DM085	F	22.59	23.61	21.75	23.50	22.07	3.27	22.54	23.85	21.54	23.56	21.97	3.27
DM086	F	28.98	28.67	29.23	28.52	29.14	2.89	29.06	28.51	29.29	28.72	29.45	2.99
DM087	F	30.03	27.85	30.89	29.10	31.48	3.83	28.90	28.33	28.98	29.03	29.17	2.88
DM088	M	32.85	32.60	33.07	32.62	32.84	6.78	31.82	31.25	32.44	30.76	31.80	5.56
DM089	F	31.65	29.25	32.79	29.36	33.73	5.28	31.28	29.09	32.24	28.83	33.14	4.82
DM090	F	25.68	25.93	25.31	26.31	25.36	0.27	25.31	26.27	24.55	26.56	24.83	0.61
DM091	M	33.79	33.38	34.02	33.27	34.01	7.67	33.92	33.56	34.34	32.70	34.17	7.69
DM092	F	35.60	35.32	35.91	35.13	35.54	9.47	35.56	34.81	35.93	34.96	36.06	9.44
DM093	F	34.63	34.29	34.71	34.72	34.87	8.64	35.06	34.68	35.32	34.63	35.35	8.99
DM094	F	25.67	26.24	25.11	26.64	25.28	0.37	26.44	26.60	25.89	27.59	27.14	0.80
DM095	F	26.99	26.32	27.27	26.86	27.46	0.98	25.66	24.26	26.38	24.73	26.60	1.25
DM096	M	25.21	22.69	26.64	23.14	26.74	2.14	26.67	25.06	27.37	26.30	27.06	1.02
DM097	F	31.44	31.69	31.46	31.40	31.25	5.45	31.20	31.22	31.16	31.34	31.10	5.20
DM098	M	30.14	29.29	30.69	28.98	31.15	4.03	28.78	28.44	28.80	28.49	29.25	2.74
DM099	F	28.85	29.51	28.37	29.52	28.52	2.98	27.00	27.64	26.13	28.26	26.66	1.17
DM100	F	30.76	30.57	30.82	30.55	30.85	4.70	30.55	30.36	30.69	30.12	30.87	4.51
DM101	F	25.13	25.07	24.91	25.48	24.99	0.89	24.84	25.43	24.05	26.40	24.46	0.92
DM102	F	28.10	28.07	27.98	28.07	28.54	2.16	28.52	28.42	28.46	28.42	29.56	2.71
DM103	F	29.82	31.15	28.64	31.97	28.66	4.10	29.76	30.76	28.74	31.57	29.24	4.08
DM104	F	28.34	28.10	27.97	28.92	28.66	2.41	29.75	28.83	29.77	30.01	30.29	3.73
DM105	F	24.30	24.52	23.62	25.33	24.60	1.48	24.61	24.50	24.37	24.59	24.71	1.45
DM106	F	30.44	29.28	30.87	29.69	31.56	4.35	30.40	29.12	30.93	29.57	31.46	4.27
DM107	M	29.53	28.85	29.82	29.07	29.36	3.28	27.88	27.29	28.00	27.73	27.72	1.69
DM108	F	29.02	28.88	28.90	29.12	29.07	3.00	28.54	27.24	29.15	27.59	29.68	2.41
DM109	F	33.36	32.87	33.53	33.17	33.95	7.38	32.76	32.51	32.91	32.55	33.36	6.83
DM110	F	23.80	24.84	22.67	25.31	22.96	2.06	26.56	27.00	25.85	27.46	26.41	0.68
DM111	F	27.89	29.71	26.27	30.56	26.48	2.25	27.30	29.47	25.57	30.00	25.89	1.80
DM112	M	25.14	26.06	24.05	26.34	24.86	0.67	25.36	25.41	24.65	26.30	25.13	0.63
DM113	F	27.43	26.89	27.31	27.71	27.80	1.43	26.40	27.47	25.37	27.77	25.94	0.80
DM114	F	28.81	29.46	27.99	29.96	28.27	2.92	29.28	29.73	28.56	30.25	28.89	3.36
DM115	F	30.15	29.76	30.29	29.90	31.82	4.44	30.47	29.03	31.26	28.64	32.06	4.25
DM116	F	32.31	31.82	32.65	31.81	32.32	6.15	32.06	31.56	32.34	31.65	32.31	5.96
DM117	F	25.42	25.56	25.04	25.74	25.34	0.58	24.57	23.95	24.18	24.83	25.09	1.49
DM118	M	31.25	30.32	31.72	30.48	32.56	5.27	32.27	31.07	32.98	31.21	33.92	6.29
DM119	F	33.02	32.91	33.19	32.32	33.43	6.96	33.69	33.65	33.64	33.69	33.73	7.68
DM120	F	32.73	31.99	33.10	32.57	33.44	6.77	32.28	31.07	33.00	30.97	33.34	6.09
DM121	F	33.47	33.60	33.81	32.77	33.60	7.44	33.13	32.15	33.81	32.54	33.49	7.00
DM122	F	26.18	25.55	26.19	26.00	27.34	0.74	25.82	25.98	25.48	26.10	26.54	0.34

TABLE 5. Data analysis of control group.

Subject	Gender	General	Right Foot					Left Foot					
			LCA	LPA	MCA	MPA	TCI	General	LCA	LPA	MCA	MPA	TCI
CG001	M	25.91	26.02	25.43	26.31	25.84	0.12	25.45	25.87	25.36	26.08	24.83	0.46
CG002	M	28.01	27.63	27.77	28.09	28.40	1.97	28.08	27.73	28.39	28.52	27.71	2.09
CG003	M	29.59	30.08	29.12	30.21	29.74	3.79	29.45	30.13	29.05	30.17	28.93	3.57
CG004	F	27.82	27.80	27.31	28.76	27.28	1.79	27.16	26.94	26.15	29.16	26.48	1.18
CG005	F	26.22	26.35	25.65	26.80	26.25	0.29	26.75	26.80	26.89	27.39	26.16	0.81
CG006	F	26.53	27.32	25.79	27.76	26.27	0.78	26.88	27.53	26.57	27.92	26.11	1.03
CG007	F	26.12	25.93	25.69	26.62	26.24	0.21	26.43	26.49	26.94	26.06	26.10	0.57
CG008	F	24.39	23.17	24.72	23.51	25.08	1.88	24.67	24.05	24.38	23.54	24.98	1.76
CG009	M	24.71	23.78	24.32	24.87	25.51	1.38	24.97	24.21	25.71	24.96	24.54	1.15
CG010	M	26.98	27.29	26.37	28.14	26.85	1.17	26.80	26.74	26.67	27.51	26.42	0.83
CG011	F	26.26	25.87	26.18	26.20	26.41	0.38	26.00	25.89	26.01	26.16	25.70	0.22
CG012	F	27.97	29.02	27.18	29.04	27.65	2.22	27.61	28.54	27.76	29.44	26.55	2.07
CG013	M	26.30	26.42	25.78	26.71	26.45	0.34	26.77	27.27	26.24	27.32	26.14	0.74
CG014	M	28.50	27.72	28.77	28.08	29.42	2.50	28.45	27.97	29.00	28.27	28.53	2.44
CG015	M	29.10	28.87	29.21	28.95	29.41	3.11	28.84	29.04	28.85	29.17	28.64	2.92
CG016	M	27.02	27.20	26.71	27.72	26.71	1.09	27.72	27.52	27.94	27.97	27.58	1.75
CG017	F	24.10	24.26	23.72	24.23	24.11	1.92	23.99	23.77	23.93	24.11	23.77	2.11
CG018	M	26.95	26.38	26.84	26.77	27.78	0.94	27.23	26.47	27.71	27.12	27.06	1.09
CG019	F	26.53	25.81	26.58	26.41	27.24	0.66	25.90	26.06	25.72	26.60	25.30	0.19
CG020	F	23.58	23.76	23.12	24.10	23.31	2.43	23.55	23.84	23.04	24.14	23.04	2.48
CG021	M	25.20	25.49	24.60	26.20	24.68	0.76	25.52	25.17	25.87	25.65	25.20	0.61
CG022	M	24.57	25.13	23.53	26.44	24.04	1.23	24.96	25.70	25.02	26.12	24.17	0.75
CG023	F	24.24	24.56	23.62	25.67	23.35	1.70	24.88	25.08	24.62	25.71	24.50	1.02
CG024	F	26.51	27.24	25.84	27.90	25.77	0.70	26.20	26.43	25.25	27.72	25.58	0.58
CG025	M	27.62	27.63	27.30	27.66	27.58	1.54	27.66	27.17	27.95	27.50	27.60	1.55
CG026	M	27.64	27.52	27.39	28.06	27.86	1.71	27.63	27.27	28.04	27.68	27.51	1.63
CG027	M	26.26	25.78	26.29	25.96	26.41	0.49	26.75	25.87	27.38	26.02	26.94	0.86
CG028	M	26.48	26.61	25.84	27.35	26.42	0.55	26.10	26.21	26.11	26.83	25.45	0.32
CG029	F	26.13	26.12	26.02	26.25	25.76	0.13	25.52	25.84	25.27	25.89	25.14	0.46
CG030	M	26.58	26.82	26.17	27.36	26.12	0.62	26.61	26.79	26.28	27.51	26.21	0.70
CG031	M	27.64	27.57	27.56	27.53	27.73	1.60	27.38	27.22	27.37	27.43	27.29	1.33
CG032	M	26.99	26.50	26.93	26.91	27.33	0.92	27.01	26.08	27.58	26.95	26.99	0.91
CG033	M	28.60	28.88	28.06	29.35	28.31	2.65	28.62	28.38	28.69	29.49	28.14	2.68
CG034	M	28.13	26.75	28.52	27.43	29.12	1.95	28.06	26.42	29.22	27.39	28.34	1.85
CG035	M	27.15	26.22	27.22	26.88	27.20	0.88	27.63	26.33	28.11	26.99	27.92	1.34
CG036	M	26.76	26.92	26.27	27.39	26.37	0.74	25.86	26.26	25.21	26.60	25.30	0.34
CG037	M	28.84	28.24	29.04	28.33	29.13	2.69	28.67	28.51	28.91	28.60	28.63	2.66
CG038	M	26.64	26.42	26.50	26.39	26.38	0.43	26.09	25.51	25.96	26.06	25.96	0.34
CG039	M	29.61	28.88	29.96	28.84	30.54	3.56	29.12	27.97	29.79	28.17	29.66	2.90
CG040	M	28.74	28.32	28.46	29.09	29.20	2.77	28.97	28.75	29.22	29.10	28.73	2.95
CG041	F	27.11	27.15	26.94	26.95	27.06	1.03	27.61	27.64	27.21	27.45	27.48	1.44
CG042	F	25.66	25.45	25.34	26.20	25.80	0.30	25.73	25.15	25.72	25.89	25.80	0.37
CG043	M	24.87	26.03	23.78	26.72	24.16	0.99	24.47	25.59	23.90	26.14	23.48	1.22
CG044	F	22.39	23.12	21.63	23.63	21.53	3.52	22.03	22.81	21.27	23.13	21.35	3.86
CG045	M	29.04	28.12	29.29	28.56	29.85	2.96	28.52	27.82	28.97	28.19	28.63	2.40

APPENDIX

See Tables 4 and 5.

ACKNOWLEDGMENT

The author D. A. Hernandez-Contreras would like to thank the CONACYT for the financial support provided for his studies.

REFERENCES

- [1] B. B. Lahiri, S. Bagavathiappan, T. Jayakumar, and J. Philip, "Medical applications of infrared thermography: A review," *Infr. Phys. Technol.*, vol. 55, pp. 221–235, Jul. 2012.
- [2] C. B. Pereira, "Infrared thermography," in *Multi-Modality Imaging*. Cham, Switzerland: Springer, 2018, pp. 1–30.
- [3] H. Peregrina-Barreto, L. A. Morales-Hernandez, J. J. Rangel-Magdaleno, J. G. Avina-Cervantes, J. M. Ramirez-Cortes, and R. Morales-Caporal, "Quantitative estimation of temperature variations in plantar angiosomes: A study case for diabetic foot," *Comput. Math. Methods Med.*, vol. 2014, Feb. 2014, Art. no. 585306.
- [4] T. Mori, T. Nagase, K. Takehara, M. Oe, Y. Ohashi, A. Amemiya, H. Noguchi, K. Ueki, T. Kadokawa, and H. Sanada, "Morphological pattern classification system for plantar thermography of patients with diabetes," *J. Diabetes Sci. Technol.*, vol. 7, no. 5, pp. 1102–1112, 2013.
- [5] T. Nagase, H. Sanada, K. Takehara, M. Oe, S. Iizaka, Y. Ohashi, M. Oba, T. Kadokawa, and G. Nakagami, "Variations of plantar thermographic patterns in normal controls and non-ulcer diabetic patients: Novel classification using angiosome concept," *J. Plastic Reconstructive Aesthetic Surg.*, vol. 64, no. 7, pp. 860–866, 2011.
- [6] F.-J. Renero-C, "The thermoregulation of healthy individuals, overweight-obese, and diabetic from the plantar skin thermogram: A clue to predict the diabetic foot," *Diabetic Foot Ankle*, vol. 8, no. 1, 2017, Art. no. 1361298.

- [7] M. Adam, E. Y. K. Ng, S. L. Oh, M. L. Heng, Y. Hagiwara, J. H. Tan, J. W. K. Tong, and U. R. Acharya, "Automated detection of diabetic foot with and without neuropathy using double density-dual tree-complex wavelet transform on foot thermograms," *Infr. Phys. Technol.*, vol. 92, pp. 270–279, Aug. 2018.
- [8] M. Adam, "Automated characterization of diabetic foot using nonlinear features extracted from thermograms," *Infr. Phys. Technol.*, vol. 89, pp. 325–337, Mar. 2018.
- [9] R. A. del Castillo Tirado, J. A. F. López, and F. J. del Castillo Tirado, "Guía de Práctica Clínica en el Pie Diabético," in *Archivos de Medicina*, vol. 10, no. 2. London, U.K.: iMedPub LTD, 2014.
- [10] P. C. Leung, "Diabetic foot ulcers—A comprehensive review," *Surgeon*, vol. 5, no. 4, pp. 219–231, 2007.
- [11] A. W. J. M. Glaudemans, I. Uçkay, and B. A. Lipsky, "Challenges in diagnosing infection in the diabetic foot," *Diabetic Med.*, vol. 32, no. 6, pp. 748–759, 2015.
- [12] P. D. Sinwar, "The diabetic foot management—Recent advance," *Int. J. Surg.*, vol. 15, pp. 27–30, Mar. 2015.
- [13] R. G. Frykberg, T. Zgonis, D. G. Armstrong, V. R. Driver, J. M. Giurini, S. R. Kravitz, A. S. Landsman, L. A. Lavery, J. C. Moore, J. M. Schuberth, D. W. Wukich, C. Andersen, and J. V. Vanore, "Diabetic foot disorders: A clinical practice guideline (2006 revision)," *J. Foot Ankle Surg.*, vol. 45, no. 5, pp. S1–S66, 2006.
- [14] D. Hernandez-Contreras, H. Peregrina-Barreto, J. Rangel-Magdaleno, and J. Gonzalez-Bernal, "Narrative review: Diabetic foot and infrared thermography," *Infr. Phys. Technol.*, vol. 78, pp. 105–117, Sep. 2016.
- [15] A. El-Baz, X. Jiang, and J. S. Suri, *Biomedical Image Segmentation: Advances and Trends*. Boca Raton, FL, USA: CRC Press, 2016.
- [16] B. Zitová and J. Flusser, "Image registration methods: A survey," *Image Vis. Comput.*, vol. 21, no. 11, pp. 977–1000, 2003.
- [17] D. Hernandez-Contreras, H. Peregrina-Barreto, J. Rangel-Magdaleno, J. Ramirez-Cortes, and F. Renero-Carrillo, "Automatic classification of thermal patterns in diabetic foot based on morphological pattern spectrum," *Infr. Phys. Technol.*, vol. 73, pp. 149–157, Nov. 2015.
- [18] D. Hernandez-Contreras, H. Peregrina-Barreto, J. Rangel-Magdaleno, F. Orihuela-Espina, and J. Ramirez-Cortes, "Measuring changes in the plantar temperature distribution in diabetic patients," presented at the *IEEE IMTC*, 2017. [Online]. Available: <https://ieeexplore.ieee.org/abstract/document/7969699>
- [19] D. Hernandez-Contreras, H. Peregrina-Barreto, J. Rangel-Magdaleno, J. A. Gonzalez-Bernal, and L. Altamirano-Robles, "A quantitative index for classification of plantar thermal changes in the diabetic foot," *Infr. Phys. Technol.*, vol. 81, pp. 242–249, Mar. 2017.
- [20] D. Hernandez-Contreras, H. Peregrina-Barreto, J. Rangel-Magdaleno, J. Ramirez-Cortes, F. Renero-Carrillo, and G. Avina-Cervantes, "Evaluation of thermal patterns and distribution applied to the study of diabetic foot," presented at the *IEEE IMTC*, 2015. [Online]. Available: <https://ieeexplore.ieee.org/abstract/document/7151315/>
- [21] D. Hernandez-Contreras, H. Peregrina-Barreto, and J. Rangel-Magdaleno, "Similarity measures to identify changes in plantar temperature distribution in diabetic subjects," presented at the *ROPEC*, 2015. [Online]. Available: <https://ieeexplore.ieee.org/abstract/document/8661366>
- [22] D. A. Hernandez-Contreras, H. Peregrina-Barreto, J. De Jesus Rangel-Magdaleno, and F. Orihuela-Espina, "Statistical approximation of plantar temperature distribution on diabetic subjects based on beta mixture model," *IEEE Access*, vol. 7, pp. 28383–28391, 2019.
- [23] N. Kaabouch, W.-C. Hu, and Y. Chen, "Alternative technique to asymmetry analysis-based overlapping for foot ulcer examination: Scalable scanning," *J. Diabetes Metabolism*, vol. 1, pp. 1–6, Jan. 2012.
- [24] N. Kaabouch, Y. Chen, J. Anderson, F. Ames, and R. Paulson, "Asymmetry analysis based on genetic algorithms for the prediction of foot ulcers," *Proc. SPIE*, vol. 7243, Jan. 2009, Art. no. 724304.
- [25] N. Kaabouch, Y. Chen, W.-C. Hu, J. Anderson, F. Ames, and R. Paulson, "Early detection of foot ulcers through asymmetry analysis," *Proc. SPIE*, vol. 7262, Feb. 2009, Art. no. 72621L.
- [26] N. Kaabouch, W.-C. Hu, Y. Chen, J. W. Anderson, F. Ames, and R. Paulson, "Predicting neuropathic ulceration: Analysis of static temperature distributions in thermal images," *J. Biomed. Opt.*, vol. 15, no. 6, 2010, Art. no. 061715.
- [27] N. Kaabouch, Y. Chen, W.-C. Hu, J. W. Anderson, F. Ames, and R. Paulson, "Enhancement of the asymmetry-based overlapping analysis through features extraction," *J. Electron. Imag.*, vol. 20, no. 1, 2011, Art. no. 013012.
- [28] C. Liu, F. van der Heijden, M. E. Klein, J. G. van Baal, S. A. Bus, and J. J. van Netten, "Infrared dermal thermography on diabetic feet soles to predict ulcerations: A case study," presented at the *Proc. SPIE*, 2013. [Online]. Available: https://www.spiedigitallibrary.org/conference-proceedings-of-spie/8572/85720N/Infrared-dermal-thermography-on-diabetic-feet-soles-to-predict-ulcerations/10.1117/12.2001807.full?casa_token=vN3rmCANPtgAAAAA
- [29] V. Check, S. S. Luan, M. Burge, C. Carranza, P. Soliz, E. McGrew, and S. Barriga, "Quantitative early detection of diabetic foot," presented at the *ACM BCB*, 2013. [Online]. Available: <https://dl.acm.org/citation.cfm?id=2506598>
- [30] G. L. Nandagopan and A. B. Haripriya, "Implementation and comparison of two image segmentation techniques on thermal foot images and detection of ulceration using asymmetry," presented at the *ICCS*, 2016. [Online]. Available: <https://ieeexplore.ieee.org/abstract/document/7754155>
- [31] T. W. Ridler, "Picture thresholding using an iterative selection method," *IEEE Trans. Syst., Man, Cybern.*, vol. SMC-8, no. 8, pp. 630–632, Aug. 1978.
- [32] J. N. Kapur, P. K. Sahoo, and A. K. C. Wong, "A new method for gray-level picture thresholding using the entropy of the histogram," *Comput. Vis., Graph., Image Process.*, vol. 29, no. 3, pp. 273–285, 1985.
- [33] W.-H. Tsai, "Moment-preserving thresholding: A new approach," *Comput. Vis., Graph., Image Process.*, vol. 29, no. 3, pp. 377–393, 1985.
- [34] V. Check, P. Soliz, E. McGrew, S. Barriga, M. Burge, and S. Luan, "Computer aided diagnosis of diabetic peripheral neuropathy," presented at the *Proc. SPIE*, 2013, doi: [10.1117/12.2043286](https://doi.org/10.1117/12.2043286).
- [35] J. J. van Netten, "Diagnostic values for skin temperature assessment to detect diabetes-related foot complications," *Diabetes Technol. Therapeutics*, vol. 16, no. 11, pp. 714–721, 2014.
- [36] T. F. Chan and L. A. Vese, "Active contours without edges," *IEEE Trans. Image Process.*, vol. 10, no. 2, pp. 266–277, Feb. 2001.
- [37] L. Vilcahuaman, R. Harba, R. Canals, M. Zequera, C. Wilches, M. T. Arista, L. Torres, and H. Arbañil, "Automatic analysis of plantar foot thermal images in at-risk type II diabetes by using an infrared camera," presented at the *IFMBE*, Jun. 2015. [Online]. Available: https://link.springer.com/chapter/10.1007/978-3-319-19387-8_55
- [38] L. Vilcahuaman, R. Harba, R. Canals, M. Zequera, C. Wilches, M. T. Arista, L. Torres, H. Arbañil, "Detection of diabetic foot hyperthermia by infrared imaging," presented at the *EMBC*, 2014. [Online]. Available: <https://ieeexplore.ieee.org/abstract/document/6944705>
- [39] L. Vilcahuaman, A. Davila, Y. Pandzic, C. Rosado, and M. Alpiste, "Analysis and experimentation of plantar foot segmentation from thermographic digital images for preventive diagnosis of diabetic foot," presented at the *IFMBE*, Jun. 2015. [Online]. Available: https://link.springer.com/chapter/10.1007/978-3-319-19387-8_388
- [40] C. Liu, J. J. van Netten, J. G. van Baal, S. A. Bus, and F. van der Heijden, "Automatic detection of diabetic foot complications with infrared thermography by asymmetric analysis," *J. Biomed. Opt.*, vol. 20, no. 2, 2015, Art. no. 026003.
- [41] J. Gauci, O. Falzon, K. P. Camilleri, C. Formosa, A. Gatt, C. Ellul, S. Mizzi, A. Mizzi, K. Cassar, and N. Chockalingam, "Automated segmentation and temperature extraction from thermal images of human hands, shins and feet," presented at the *MEDICON*, 2016. [Online]. Available: https://link.springer.com/chapter/10.1007/978-3-319-32703-7_55
- [42] L. Fraiwan, M. AlKhodari, J. Ninan, B. Mustafa, A. Saleh, and M. Ghazal, "Diabetic foot ulcer mobile detection system using smart phone thermal camera: A feasibility study," *BioMed. Eng. OnLine*, vol. 16, no. 11, 2017, Art. no. 117.
- [43] B. G. Sudha, V. Umadevi, and J. M. Shivaram, "Thermal image acquisition and segmentation of human foot," presented at the *SPIN*, 2017. [Online]. Available: <https://ieeexplore.ieee.org/abstract/document/8049920/>
- [44] B. G. Sudha, V. Umadevi, J. M. Shivaram, M. Y. Sikkandar, A. Al Amoudi, and H. C. Chaluvanarayana, "Statistical analysis of surface temperature distribution pattern in plantar foot of healthy and diabetic subjects using thermography," presented at the *ICCS*, 2018. [Online]. Available: <https://ieeexplore.ieee.org/abstract/document/8524310/>
- [45] M. Etehdadtavakol, E. Y. K. Ng, and N. Kaabouch, "Automatic segmentation of thermal images of diabetic-at-risk feet using the snakes algorithm," *Infr. Phys. Technol.*, vol. 86, pp. 66–76, Nov. 2017.
- [46] A. Bougrine, R. Harba, R. Canals, R. Ledee, and M. Jabloun, "A joint snake and atlas-based segmentation of plantar foot thermal images," presented at the *IPTA*, 2017. [Online]. Available: <https://ieeexplore.ieee.org/abstract/document/8310081>

- [47] M. S. Prabhu and S. Verma, "Comparative analysis of segmentation techniques for progressive evaluation and risk identification of diabetic foot ulcers," presented at the *ICBDSC*, 2019. [Online]. Available: <https://ieeexplore.ieee.org/abstract/document/8645591>
- [48] K. Zhang, L. Zhang, H. Song, and W. Zhou, "Active contours with selective local or global segmentation: A new formulation and level set method," *Image Vis. Comput.*, vol. 28, no. 4, pp. 668–676, 2010.
- [49] F. Dong, Z. Chen, and J. Wang, "A new level set method for inhomogeneous image segmentation," *Image Vis. Comput.*, vol. 31, no. 10, pp. 809–822, Oct. 2013.
- [50] B. N. Li, J. Qin, R. Wang, M. Wang, and X. Li, "Selective level set segmentation using fuzzy region competition," *IEEE Access*, vol. 4, pp. 4777–4788, Aug. 2016.
- [51] M. B. Salah, A. Mitiche, and I. B. Ayed, "Multiregion image segmentation by parametric kernel graph cuts," *IEEE Trans. Image Process.*, vol. 20, no. 2, pp. 545–557, Feb. 2011.
- [52] M. Kass, A. Witkin, and D. Terzopoulos, "Snakes: Active contour models," *Int. J. Comput. Vis.*, vol. 1, no. 4, pp. 321–331, 1988.
- [53] A. Klein, D.-J. Kroon, Y. Hoogeveen, L. J. S. Kool, W. K. J. Renema, and C. H. Slump, "Multimodal image registration by edge attraction and regularization using a B-spline grid," presented at the *Proc. SPIE*, 2019, doi: [10.1117/12.2078267](https://doi.org/10.1117/12.2078267).
- [54] *Thermography Guidelines: Standards and Protocols in Clinical Thermographic Imaging*, Int. Acad. Clin. Thermol., Redwood City, CA, USA, 2002.
- [55] S. Bagavathiappan, J. Philip, T. Jayakumar, B. Raj, P. N. S. Rao, M. Varalakshmi, and V. Mohan, "Correlation between plantar foot temperature and diabetic neuropathy: A case study by using an infrared thermal imaging technique," *J. Diabetes Sci. Technol.*, vol. 4, no. 6, pp. 1386–1392, Nov. 2010.
- [56] A. W. Chan, I. A. MacFarlane, and D. R. Bowsher, "Contact thermography of painful diabetic neuropathic foot," *Diabetes Care*, vol. 14, no. 10, pp. 918–922, 1991.
- [57] P. C. Sun, H.-D. Lin, S.-H. E. Jao, Y.-C. Ku, R.-C. Chan, and C.-K. Cheng, "Relationship of skin temperature to sympathetic dysfunction in diabetic at-risk feet," *Diabetes Res. Clin. Pract.*, vol. 73, no. 1, pp. 41–46, 2006.



DANIEL ALEJANDRO HERNANDEZ-CONTRERAS was born in Puebla, Mexico. He received the B.Sc. degree in mechatronic engineering from the Popular Autonomous University of Puebla State (UPAEP), Mexico, and the M.Sc. degree in electronics from the National Institute of Astrophysics, Optics, and Electronics (INAOE), Mexico. He is currently pursuing the Ph.D. degree in electronics with INAOE. His research interest includes image and signal processing.



HAYDE PEREGRINA-BARRETO received the B.Sc. degree in computer engineering from the Instituto Tecnológico de Cuautla, Mexico, in 2006, the M.Sc. degree in engineering from the Universidad de Guanajuato, Mexico, in 2008, and the Ph.D. degree in engineering from the Universidad Autónoma de Querétaro, Mexico, in 2011. She is currently a full-time Researcher with the Computer Science Department, INAOE, Mexico. Her research interests include clinical thermography, medical image analysis, and computer vision. She is a member of the Mexican National Research System (SNI) level 1.



JOSE DE JESUS RANGEL-MAGDALENO received the B.E. degree in electronics engineering and the M.E. degree in electrical engineering on hardware signal processing from the Universidad de Guanajuato, Mexico, in 2006 and 2008, respectively, and the Ph.D. degree from the Universidad Autónoma de Querétaro, Mexico, in 2011. He is currently a full-time Researcher with the Electronics Department, INAOE, Mexico. His research interests include FPGAs, signal and image processing, instrumentation and mechatronics. He is a member of the Mexican National Research System (SNI), level 1.



FRANCISCO JAVIER RENERO-CARRILLO received the bachelor's degree in physics from the Universidad Autónoma de Puebla, Mexico, in 1987, and the M.E. and Ph.D. degrees from Osaka University, in 1992 and 1995, respectively. He is currently a full-time Researcher with the Optics Department, INAOE, Mexico. His research interest includes in optical image processing for medical applications.

• • •